

Charged excitons and biexcitons bound to isoelectronic centersS. Marcet,¹ C. Ouellet-Plamondon,¹ G. Éthier-Majcher,¹ P. Saint-Jean,¹ R. André,² J. F. Klem,³ and S. Francoeur^{1,*}¹*Département de Génie Physique, École Polytechnique de Montréal, Montréal, Québec, Canada H3C 3A7*²*Nanophysics and Semiconductor Group, Institut Néel, CEA/CNRS/Université Joseph Fourier,**25 rue des Martyrs, 38042 Grenoble, France*³*Sandia National Laboratory, Albuquerque, New Mexico 87185, USA*

(Received 13 October 2010; published 7 December 2010)

We demonstrate that the singular binding mechanism characterizing isoelectronic centers formed from two isoelectronic traps can also bind, in addition to the well-studied excitons, various number of charges. Using the emission fine structure of Te dyads in ZnSe and N dyads in GaAs, we establish that these pseudodonor and pseudoacceptor can bind positively and negatively charged excitons, respectively, and that both can bind biexcitons. This ability to bind various charge configurations, in addition to their very low inhomogeneous broadenings and perfectly defined symmetries, further establishes isoelectronic centers as an interesting alternative to epitaxial quantum dots for a number of applications.

DOI: [10.1103/PhysRevB.82.235311](https://doi.org/10.1103/PhysRevB.82.235311)

PACS number(s): 78.67.Hc, 78.55.-m

I. INTRODUCTION

Isoelectronic centers, or more precisely isovalent impurities forming excitonic bound states,¹ allow forming various molecular-sized quantum emitters in semiconductors.²⁻⁶ Just like epitaxial or colloidal quantum dots formed from 10^4 to 10^6 atoms, their emission can be tuned by changing the number of impurities involved and their respective interatomic separations in the host lattice. However, these lesser known nanostructures offer a number of unique characteristics that larger quantum dots may never achieve. In a regime where the quantum emitter is composed of very few atoms whose respective positions are rigidly set by the host lattice, the inhomogeneous broadening associated with a particular atomic configuration of atoms can be extremely small, even when measured on large ensembles.^{2,7,8} As the control over the composition, size, and shape of quantum dots is relatively poor, the ability to fabricate ensembles of identical emitters or a single emitter whose emission is precisely controlled is a considerable advantage for most applications, from quantum dot lasers to cavity quantum electrodynamics.⁹ Furthermore, the symmetry of isoelectronic centers is perfectly defined,^{2,5,7} allowing to take full advantage its influence on electronic states, an aspect that has remained difficult to exploit with quantum dots.

Although these advantages over quantum dots are highly desirable, it remained to be demonstrated that the binding mechanisms at play in isoelectronic centers allowed binding multiple charge configurations. Indeed, in recent years, a number of promising applications based on charged excitons and biexcitons have emerged. Charged excitons provide a convenient and efficient way to initialize the spin of electrons and holes and manipulate their wave functions¹⁰⁻¹³ and, through their emission cascade, biexcitons bound to nanostructures of relatively high symmetry are a promising way to generate single pairs of entangled photons.^{14,15}

In this Letter, we demonstrate that isoelectronic Te dyads and N dyads can also bind charged excitons and biexcitons. This new aspect of isoelectronic centers, combined with the absence of inhomogeneous broadening, may be extremely

advantageous for scaling up recent advances in quantum computing using semiconducting nanostructures. Also, isoelectronic centers would be perfect candidates for the realization of entangled photons source that do not require manual selection or complex growth procedures.

Isovalent substitutions always create localized singularities in the host electronic charge density. If the electronegativity and size differences between the two atoms involved are important, such singularity can trap an itinerant carrier.^{2,16} A pseudoacceptor (GaAs:N, GaP:N) attracts and traps an electron while a pseudodonor (GaP:Bi, ZnSe:Te) traps a hole. This primary particle, tightly localized in a volume which is about the size of a unit cell,^{16,17} can then bind a particle of the opposite charge through Coulomb interaction, resulting in a bound exciton. Although it has been shown that N atoms could bind biexcitons in GaP,¹⁸ binding of multiple charge configurations has never been demonstrated experimentally nor considered theoretically.

The samples investigated were both grown on GaAs substrates by molecular beam epitaxy. The first one consists of a Te delta-doped ZnSe layer inserted between two 40-nm-thick ZnSe layers. The estimated density of Te atoms is $2500 \mu\text{m}^{-2}$. This corresponds to a dyad concentration of $4 \mu\text{m}^{-2}$. The structure of the second sample consists of a 25 nm GaAs:N layer, clad by a protective 5 nm of GaAs on both sides, and sandwiched between two $\text{Al}_{0.25}\text{Ga}_{0.75}\text{As}$ barriers. The nitrogen dyad concentration was measured at $0.5 \mu\text{m}^{-2}$. The microphotoluminescence measurements were performed at 4.5 K in a custom-made confocal microscope.¹⁹ Excitation is performed at 405 nm (ZnSe) or 780 nm (GaAs) and the overall spectral resolution is approximately 300 and $70 \mu\text{eV}$ at these wavelengths. This microscope provides a spatial resolution of $0.82 \mu\text{m}$, allowing to probe the PL from single dyads. A magnetic field of up to 6 T can be applied in a Faraday configuration.

II. ZnSe:Te

Dyads formed from pseudodonor Te impurities create a number of bound states in ZnSe whose emission occurs in a

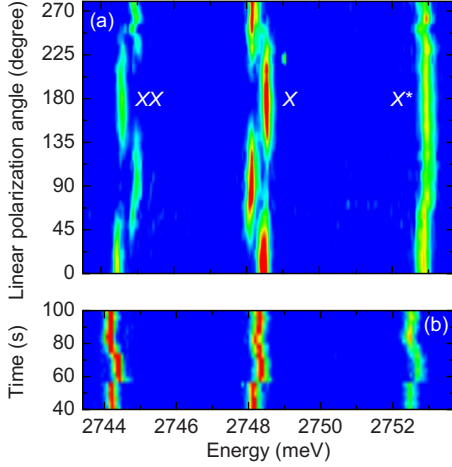


FIG. 1. (Color online) Photoluminescence from a Te dyad of C_{2v} symmetry in ZnSe. (a) Intensity as function of energy and polarization angle. (b) Intensity as a function of time and energy for transitions linearly polarized along 0° .

range extending from 2720 to 2780 meV.⁶ Dyads appears to be of C_{2v} symmetry with several distinct interatomic separations.²⁰ Panel (a) of Fig. 1 presents the intensity of the photoluminescence as a function of emission energy and polarization angle for a single Te dyad. The emission is composed of four linearly polarized transitions accompanied at higher energy, as will be determined later on, by two degenerate and circularly polarized transitions. The energy separation between these three groups of transitions is roughly 4 meV. The strictly identical spectral diffusion observed from the six transitions as a function of time [see panel (b)] confirms that these transitions most likely originate from the same dyad. Te dyads often exhibit intensity fluctuations and spectral diffusions resulting from charges trapped in the vicinity of the dyad.²⁰

Although the exact interatomic separation is not known, the presence of linearly polarized transitions along $[110]$ (0°) and $[\bar{1}\bar{1}0]$ (90°) crystallographic directions reveals that this dyad is of C_{2v} symmetry and located in a plane perpendicular to the wave vector of the emitted light.^{20,21} The four polarized transitions look somewhat similar to what would have been expected if both heavy- and light-hole excitonic transitions were simultaneously observed,^{5,20} but, due to the compressive strain created on the ZnSe host by the GaAs substrate, light-hole transitions, pushed approximately 12.6 meV to higher energy,²² were not observed in this work.^{6,20} For reasons presented below, only two of these four transitions are associated with excitonic states, the other two involve a biexcitonic state, and the two degenerate transitions are assigned to a charged exciton.

The excitonic or biexcitonic origin of optical transitions is usually determined from the variation in the emitted intensity as a function of the excitation intensity. For both quantum dots²³ and isoelectronic nitrogen,¹⁸ the integrated intensity (I) can be represented by a power law of the excitation density (P) as $I \propto P^k$. The exponent for the biexciton (k_{XX}) should be twice that of the exciton (k_X), and, ideally, $k_X = 1$. Panel (a) of Fig. 2 presents the variation in the emitted in-

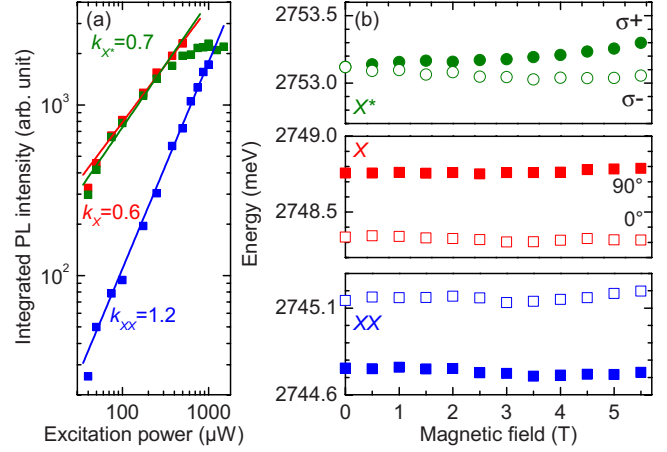


FIG. 2. (Color online) Photoluminescence from excitons X , biexcitons XX , and charged excitons (X^*) bound to a Te dyad of C_{2v} symmetry in ZnSe. (a) Integrated intensity as a function of the excitation power. (b) Energy as a function of magnetic field in Faraday configuration.

tensity as a function of excitation intensity. We find $k_X = 0.6$, $k_{XX} = 1.2$, and $k_{X^*} = 0.7$. The factor of 2 between k_X and k_{XX} allows the identification of the biexcitonic and excitonic transitions. As expected from the work done on quantum dots, the exponent for the charged exciton is very similar to that of the exciton. Measured on a number of similar dyads, k_X varies from 0.6 to 0.8. Although there is some uncertainty on the value of the exponent (~ 0.1), it clearly appears that k_X and k_{X^*} are smaller than one. Despite this low coefficient, k_{XX} is always twice as large as k_X . Although not well understood at this time, this low value suggests that new recombination channels become available in the vicinity of the dyad as the excitation power is increased.

In strained ZnSe, the degeneracy between heavy and light hole is lifted and, just like the case of semiconductor quantum dots, only heavy holes need to be considered. In C_{2v} symmetry, electrons and heavy-holes transform as Γ_5 .²⁴ According to their integral spin, exciton, and biexciton representations are single valued. In C_{2v} , the degeneracy of all four excitonic states, Γ_{1-4} , is lifted by the exchange and crystal field interaction. The four states result in two optically allowed transitions and radiative emission from Γ_2 and Γ_4 result in transitions linearly polarized along and perpendicular to the dyad.²⁰ Assuming both electrons and both holes forming the biexciton are in their lowest energy state, the wave functions of both pairs of identical particles must be antisymmetric and the lowest energy state of the biexciton must therefore transform as Γ_1 . The emission cascade from the biexciton to the ground state (Γ_1) can occur through either excitonic states: $\Gamma_1 \rightarrow \Gamma_2 \rightarrow \Gamma_1$ or $\Gamma_1 \rightarrow \Gamma_4 \rightarrow \Gamma_1$. According to this recombination scheme, the polarization ordering between the two pairs of transitions will be reversed, as observed in panel (a) of Fig. 1. Furthermore, since both recombination paths share the same initial and final states, the splitting between the exciton and the biexciton doublet should be the same. Indeed, for all dyads studied, the splitting is found to be identical.

The energy of all transitions under a magnetic field in Faraday configuration is presented in panel (b) of Fig. 2. All

transitions exhibit a linear and quadratic shift due to the Zeeman effect and diamagnetic shift, respectively. Excitonic and biexcitonic transitions mostly remain linearly polarized but begin to depolarize at high fields. The degeneracy of the line at higher energy is lifted and its emission is circularly polarized at all fields.

Although such degenerate transition could originate from an exciton bound to a dyad of D_{2d} or C_{3v} symmetry, we rule out this possibility for two reasons. First, a systematic study of more than 50 dyads did not reveal any dyad of symmetry other than C_{2v} .²⁰ Second, this degenerate transition is always accompanied by two linearly polarized transitions associated to an exciton or by four linearly polarized transitions associated to an exciton and a biexciton. The systematic presence of the linearly polarized transitions is incompatible with any other symmetry than C_{2v} . Therefore, this degenerate transition can only result from the absence of exchange interaction associated with a negatively or positively charged exciton.

The measured diamagnetic shifts are $\gamma^X=0.9\pm 0.2$, $\gamma^{XX}=1.6\pm 0.3$, and $\gamma^*=1.3\pm 0.2 \mu\text{eV T}^{-2}$. For all states observed, the exciton diamagnetic shift is small compared to that of other types of bound excitons in ZnSe,^{25–27} indicating a strong localization of all charged carriers involved.

The charged exciton appears to be positively charged for two reasons. (i) Treating the Coulomb interaction between the exciton and its extra charge as a perturbation to single-particle states, we expect the binding energy of the negatively charged exciton to exceed that of the exciton since the attraction between the tightly localized hole and the electron is stronger than the repulsion between both electrons. Using a similar reasoning, we expect the binding energy of the exciton to exceed that of the positively charged exciton since the repulsion between two localized holes should be important. (ii) A negatively charged exciton would, after recombination of the exciton, leave behind a free electron. Due to a significant change in wave function localization, the measured diamagnetic shift of X^* would then be reduced with respect to that of the exciton.^{28,29} Since γ^* is equal or at most slightly exceeds γ^X , the remaining charge is bound to the Te dyad. As an electron alone cannot be bound, we assign the X^* to a positively charged exciton.

The binding energy of the biexciton is positive, indicating that the attraction energy between an electron and a localized hole is greater than the repulsion energy between electrons, as can be expected considering the important localization of the hole with respect to the electron. Finally, γ^{XX} is slightly higher than that of both other transitions and indicates that the spatial extent of the second exciton exceeds the first one.

Figure 3 shows the relative biexciton and charged exciton binding energies as a function of the exciton emission energy. $E_X - E_{XX/X^*}$ represents the energy necessary to bind additional charges on a dyad. Both complexes exhibit an increase of their binding energy as a function of the emission energy. Since the emission energy increases with the interatomic separation of the dyads,^{2,30} these results suggest that the binding energy of both the charged exciton and the biexciton increases with the interatomic separation. This is explained by a decrease of the overlap between the wave functions of the various charges involved and a decrease of the repulsive Coulomb interaction. Interestingly, the binding en-

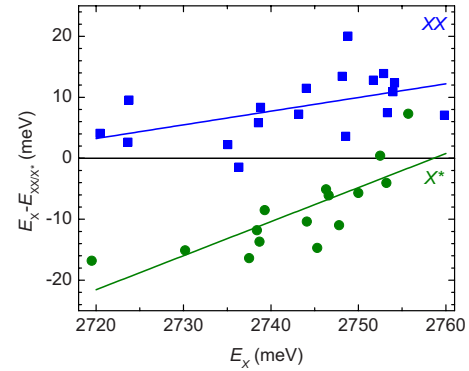


FIG. 3. (Color online) Energy emission separation of the charged excitons (green circle) and biexcitons (blue square) with the excitons as a function of the exciton energy. The exciton emission energy used is the average of the two linearly polarized excitonic transitions.

ergy of the charged exciton changes sign for dyads with large interatomic separation.

Even though we cannot clearly distinguish different configurations, several interatomic distances are likely observed and may partly explain the increase of the binding energy. Increasing the interatomic distance leads to a decrease of the wave function overlap between the carriers and to a decrease in the repulsive Coulomb interaction. The linear and continuous dependence of the binding energy shows that the origin of the inhomogeneous broadening have the same effect that the interatomic separation.

III. GaAs:N

We now demonstrate that a pseudoacceptor, a N dyad in GaAs, can bind both charged excitons and biexcitons as well. Previous work has shown that single N impurities could bind biexcitons¹⁸ but here all measurements were done on the nitrogen dyad configuration emitting closer to the band-gap energy of GaAs,³¹ corresponding either to a first or fourth anionic neighbor configuration.¹⁷ A thorough analysis of the excitonic luminescence can be found in Refs. 5 and 32. In contrast to the system described in the previous section and most other quantum structures generally studied, the heavy- and light-hole bands are degenerate and the overall number of exciton, biexciton, and charged exciton states composing the emission fine structure is considerably increased.

Panels (a) and (b) of Fig. 4 shows eight transitions. The four linearly polarized excitonic transitions at high energy indicate a dyad of C_{2v} symmetry located in the plane perpendicular to the wave vector of the emitted light. An intense doublet E_{1-2}^* , degenerate at 0 T, is located approximately 2 meV below the excitonic transitions. Although very faint, another doublet (E_{3-4}^*) is present approximately 180 μeV below. Both of these doublets are assigned to a charged exciton with an enhanced binding energy with respect to the exciton. Panel (c) of Fig. 4 shows the energy of these four states under a magnetic field. All degeneracies are lifted and all lines clearly shift to higher energy, indicating an important diamagnetic shift. Transitions $E_{3,4}^*$ are relatively weak

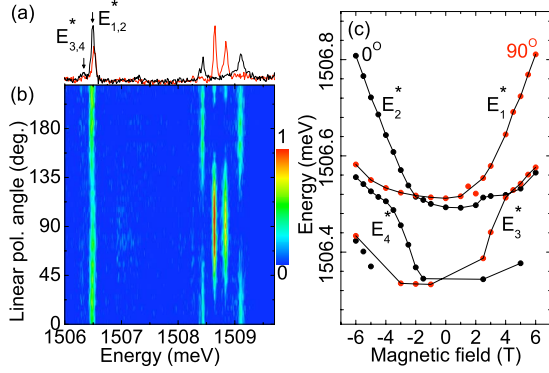


FIG. 4. (Color online) Photoluminescence intensity from an in-plane C_{2v} N dyad. (a) Polarized emission spectra taken at 0° and 90° . Arrows indicate the position of the two degenerate charged exciton transitions. (b) Intensity as a function of polarization angle and energy. (c) Energy as a function of magnetic field for the four transitions related to the charged exciton.

and although the precision of their position does not allow an elaborate analysis, the curvatures of $E_{1,3}^*$ and $E_{2,4}^*$ around ± 4 T suggest an anticrossing.

Although a larger binding energy suggests that the exciton is positively charged, this possibility is ruled out by the enhanced diamagnetic shift with respect to that of the exciton and the presence of two doublets at 0 T. Indeed, after recombination, the final state of a positively charged exciton would be a free hole and the measured diamagnetic shift would then be equal or less than that of the exciton.^{28,29} Comparing the charged exciton diamagnetic coefficient ($5.3 \pm 0.1 \mu\text{eV}/\text{T}^2$) with that of the exciton ($1.99 \pm 0.06 \mu\text{eV}/\text{T}^2$), an extra positive charge appears unlikely. For a negatively charged exciton, the two electrons form a Γ_1 spin singlet and the hole can be either heavy or light, resulting in a total of two doubly degenerate Γ_5 states. Heavy-hole charged excitons produce two circularly polarized transitions while light-hole charged excitons produce two circularly polarized transitions and two linearly polarized transitions. However, these last two transitions are inaccessible for in-plane dyads. Although heavy- and light-hole states of similar polarization are strongly mixed, two doubly degenerate states are nonetheless expected, matching the observed fine structure of the charged exciton.

To explain the enhanced binding energy with respect to that of the exciton, the second negative charge must be in a configuration minimizing the repulsion with the first tightly bound electron. Indeed, for an exciton bound to a negatively charged dyad, a configuration somewhat similar to that of an exciton bound to an ionized acceptor, the relative delocalization of the second electron with respect to the tightly bound electron could increase the overall binding energy. This interpretation is confirmed by the significant diamagnetic shift increase of the charge exciton with respect to the exciton. Finally, the considerable overlap between the second electron with the hole favors their recombination.

Panels (a) and (b) of Fig. 5 show the emission spectra measured on an out-of-plane dyad of C_{2v} symmetry. Although this dyad does not match the spectra expected from its configuration, the presence of a biexciton makes it very

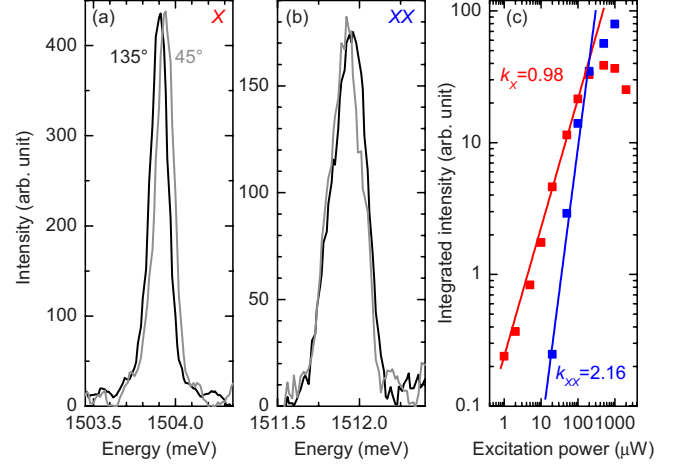


FIG. 5. (Color online) Photoluminescence from a N dyad of C_{2v} symmetry located in a (101) plane. (a) Exciton and (b) biexciton spectra. (c) PL Integrated intensity as a function of excitation power.

interesting. The emission spectra from this dyad is composed of two groups of two linearly polarized transitions separated by approximately 8 meV, which strongly exceeds the fine structure splitting generally observed.³² Panel (c) presents the integrated intensity of this emission as a function of excitation power. The variation is linear for the low-energy group of transitions and quadratic for the other. We therefore assign them to excitonic and biexcitonic emissions. As measured on biexcitons bound to individual N impurities in GaP, the binding energy of the biexciton is reduced with respect to that of the exciton.¹⁸ As expected, a polarization reversal is observed and the fine structure splittings of the exciton and biexciton are identical.

In C_{2v} symmetry, the crystal field and exchange interactions result in five excitonic and six biexcitonic states leading to optical transitions. The number of recombination pathways for the biexciton is therefore considerable. Interestingly, the exciton spectra [panel (a)] is composed of only two linearly polarized lines instead of the expected five transitions,^{21,33} indicating that for some unknown reasons three transitions are suppressed. Furthermore, a number of biexcitonic states also appear suppressed, as more than two transitions could be expected. The absence of a number of lines, added to the fact that few of the dyads measured exhibited a biexcitonic emission, probably indicate that biexciton bound to N dyads of small interatomic separations can only be observed in some particular conditions. Although only a small subset of the expected transitions is observed, the existence of the bound biexciton is confirmed.

IV. CONCLUSION

The results presented in this work establish that isoelectronic centers, just like their larger and more conventional counterparts, can bind various many-carrier configurations.

The binding mechanisms at play in these nanostructures are quite different from the extensively studied heterostructure confinement and, although a qualitative understanding of the exciton binding mechanisms exists, an adequate analysis of the binding energy of the various carrier configurations probably requires sophisticated tools rigorously taking into account carrier-carrier interactions, including exchange and correlation effects.

ACKNOWLEDGMENTS

The authors would like to acknowledge Sandia National Laboratories, a multiprogram laboratory managed and operated by Sandia Corporation, a wholly owned subsidiary of Lockheed Martin Corporation, for the U.S. Department of Energy's National Nuclear Security Administration under Contract No. DE-AC04-94AL85000.

*sebastien.francoeur@polymtl.ca

- ¹J. J. Hopfield, D. G. Thomas, and R. T. Lynch, *Phys. Rev. Lett.* **17**, 312 (1966).
- ²D. Thomas and J. Hopfield, *Phys. Rev.* **150**, 680 (1966).
- ³B. Gil and H. Mariette, *Phys. Rev. B* **35**, 7999 (1987).
- ⁴S. Francoeur, S. Nikishin, C. Jin, Y. Qiu, and H. Temkin, *Appl. Phys. Lett.* **75**, 1538 (1999).
- ⁵S. Francoeur, J. F. Klem, and A. Mascarenhas, *Phys. Rev. Lett.* **93**, 067403 (2004).
- ⁶A. Muller, P. Bianucci, C. Piermarocchi, M. Fornari, I. C. Robin, R. Andre, and C. K. Shih, *Phys. Rev. B* **73**, 081306(R) (2006).
- ⁷B. Gil, J. Camassel, J. P. Albert, and H. Mathieu, *Phys. Rev. B* **33**, 2690 (1986).
- ⁸R. T. Harley and R. M. Macfarlane, *J. Phys. C* **16**, L1121 (1983).
- ⁹A. Badolato, K. Hennessy, M. Atature, J. Dreiser, E. Hu, P. M. Petroff, and A. Imamoglu, *Science* **308**, 1158 (2005).
- ¹⁰M. Atature, J. Dreiser, A. Badolato, A. Hoge, K. Karrai, and A. Imamoglu, *Science* **312**, 551 (2006).
- ¹¹X. Xu, Y. Wu, B. Sun, Q. Huang, J. Cheng, D. G. Steel, A. S. Bracker, D. Gammon, C. Emary, and L. J. Sham, *Phys. Rev. Lett.* **99**, 097401 (2007).
- ¹²B. D. Gerardot, D. Brunner, P. A. Dalgarno, P. Ohberg, S. Seidl, M. Kroner, K. Karrai, N. G. Stoltz, P. M. Petroff, and R. J. Warburton, *Nature (London)* **451**, 441 (2008).
- ¹³D. Press, T. D. Ladd, B. Zhang, and Y. Yamamoto, *Nature (London)* **456**, 218 (2008).
- ¹⁴C. Santori, M. Pelton, G. Solomon, Y. Dale, and Y. Yamamoto, *Phys. Rev. Lett.* **86**, 1502 (2001).
- ¹⁵A. Mohan, M. Felici, P. Gallo, B. Dwir, A. Rudra, J. Faist, and E. Kapon, *Nat. Photonics* **4**, 302 (2010).
- ¹⁶R. A. Faulkner, *Phys. Rev.* **175**, 991 (1968).
- ¹⁷P. R. C. Kent and A. Zunger, *Phys. Rev. B* **64**, 115208 (2001).
- ¹⁸J. L. Merz, R. A. Faulkner, and P. J. Dean, *Phys. Rev.* **188**, 1228 (1969).
- ¹⁹S. Marcet, C. Ouellet-Plamondon, and S. Francoeur, *Rev. Sci. Instrum.* **80**, 063101 (2009).
- ²⁰S. Marcet, R. André, and S. Francoeur, *Phys. Rev. B* **82**, 235309 (2010).
- ²¹S. Francoeur and S. Marcet, *J. Appl. Phys.* **108**, 043710 (2010).
- ²²K. Shahzad, *Phys. Rev. B* **38**, 8309 (1988).
- ²³K. Brunner, G. Abstreiter, G. Bohm, G. Trankle, and G. Weimann, *Phys. Rev. Lett.* **73**, 1138 (1994).
- ²⁴G. F. Koster, J. O. Dimmock, R. G. Wheeler, and H. Statz, *Properties of the Thirty-Two Point Groups* (MIT Press, Cambridge, MA, 1963).
- ²⁵A. Hoffmann, D. Wiesmann, I. Loa, R. Heitz, U. Pohl, I. Broser, L. Worschech, E. Kurtz, D. Hommel, G. Landwehr, D. Hoffmann, and B. Meyer, *J. Cryst. Growth* **159**, 302 (1996).
- ²⁶U. Pohl, D. Wiesmann, G. Kudlek, B. Litzenburger, and A. Hoffmann, *J. Cryst. Growth* **159**, 414 (1996).
- ²⁷O. Homburg, P. Michler, K. Sebal, J. Gutowski, H. Wenisch, and D. Hommel, *J. Cryst. Growth* **214-215**, 832 (2000).
- ²⁸C. Schulhauser, D. Haft, R. J. Warburton, K. Karrai, A. O. Govorov, A. V. Kalameitsev, A. Chaplik, W. Schoenfeld, J. M. Garcia, and P. M. Petroff, *Phys. Rev. B* **66**, 193303 (2002).
- ²⁹Y. J. Fu, S. D. Lin, M. F. Tsai, H. Lin, C. H. Lin, H. Y. Chou, S. J. Cheng, and W. H. Chang, *Phys. Rev. B* **81**, 113307 (2010).
- ³⁰X. Liu, M.-E. Pistol, and L. Samuelson, *Phys. Rev. B* **42**, 7504 (1990).
- ³¹R. Schwabe, W. Seifert, F. Bugge, and R. Bindemann, *Solid State Commun.* **55**, 167 (1985).
- ³²S. Marcet, C. Ouellet-Plamondon, J. F. Klem, and S. Francoeur, *Phys. Rev. B* **80**, 245404 (2009).
- ³³D. Karaickaj, A. Mascarenhas, J. F. Klem, K. Volz, W. Stolz, M. Adamcyk, and T. Tiedje, *Phys. Rev. B* **76**, 125209 (2007).